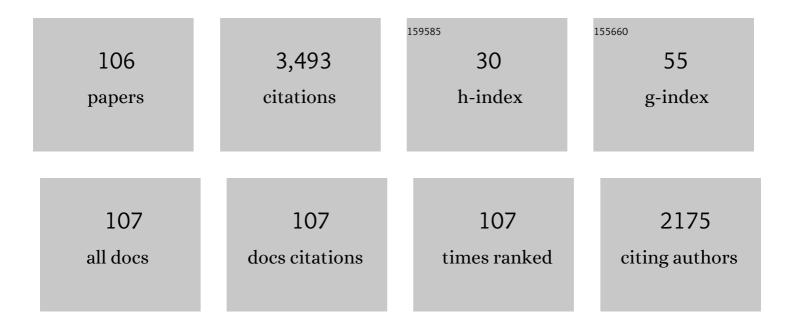
## Yang Xia

## List of Publications by Year in descending order

Source: https://exaly.com/author-pdf/9408972/publications.pdf Version: 2024-02-01



VANC VIA

#	Article	IF	CITATIONS
1	Magic-Angle Effect in Magnetic Resonance Imaging of Articular Cartilage. Investigative Radiology, 2000, 35, 602-621.	6.2	271
2	Quantitative in situ correlation between microscopic MRI and polarized light microscopy studies of articular cartilage. Osteoarthritis and Cartilage, 2001, 9, 393-406.	1.3	251
3	Relaxation anisotropy in cartilage by NMR microscopy (μMRI) at 14-μm resolution. Magnetic Resonance in Medicine, 1998, 39, 941-949.	3.0	232
4	Therapeutic Potential of Mesenchymal Cell–Derived miRNA-150-5p–Expressing Exosomes in Rheumatoid Arthritis Mediated by the Modulation of MMP14 and VEGF. Journal of Immunology, 2018, 201, 2472-2482.	0.8	211
5	Orientational dependence ofT2 relaxation in articular cartilage: A microscopic MRI (?MRI) study. Magnetic Resonance in Medicine, 2002, 48, 460-469.	3.0	202
6	Origin of cartilage laminae in MRI. Journal of Magnetic Resonance Imaging, 1997, 7, 887-894.	3.4	166
7	Diffusion and relaxation mapping of cartilage-bone plugs and excised disks using microscopic magnetic resonance imaging. Magnetic Resonance in Medicine, 1994, 31, 273-282.	3.0	145
8	Imaging the physical and morphological properties of a multi-zone young articular cartilage at microscopic resolution. Journal of Magnetic Resonance Imaging, 2003, 17, 365-374.	3.4	88
9	EGFR signaling is critical for maintaining the superficial layer of articular cartilage and preventing osteoarthritis initiation. Proceedings of the National Academy of Sciences of the United States of America, 2016, 113, 14360-14365.	7.1	83
10	Biochemical (and Functional) Imaging of Articular Cartilage. Seminars in Musculoskeletal Radiology, 2001, 05, 329-344.	0.7	80
11	Depthâ€dependent profiles of glycosaminoglycans in articular cartilage by μMRI and histochemistry. Journal of Magnetic Resonance Imaging, 2008, 28, 151-157.	3.4	67
12	Velocity and diffusion imaging in dynamic NMR microscopy. Journal of Magnetic Resonance, 1991, 91, 326-352.	0.5	66
13	Heterogeneity of cartilage laminae in MR imaging. Journal of Magnetic Resonance Imaging, 2000, 11, 686-693.	3.4	63
14	The structural adaptations in compressed articular cartilage by microscopic MRI (μMRI) T2 anisotropy. Osteoarthritis and Cartilage, 2004, 12, 887-894.	1.3	59
15	Multi-components of T2 relaxation in ex vivo cartilage and tendon. Journal of Magnetic Resonance, 2009, 198, 188-196.	2.1	55
16	The depth-dependent anisotropy of articular cartilage by Fourier-transform infrared imaging (FTIRI). Osteoarthritis and Cartilage, 2007, 15, 780-788.	1.3	54
17	Contrast in NMR imaging and microscopy. Concepts in Magnetic Resonance, 1996, 8, 205-225.	1.3	53
18	Dependencies of multi-component T2 and T1ï•relaxation on the anisotropy of collagen fibrils in bovine nasal cartilage. Journal of Magnetic Resonance, 2011, 212, 124-132.	2.1	53

#	Article	IF	CITATIONS
19	Characteristics of topographical heterogeneity of articular cartilage over the joint surface of a humeral head. Osteoarthritis and Cartilage, 2002, 10, 370-380.	1.3	52
20	Damages to the extracellular matrix in articular cartilage due to cryopreservation by microscopic magnetic resonance imaging and biochemistry. Magnetic Resonance Imaging, 2009, 27, 648-655.	1.8	49
21	Concentration profiles of collagen and proteoglycan in articular cartilage by Fourier transform infrared imaging and principal component regression. Spectrochimica Acta - Part A: Molecular and Biomolecular Spectroscopy, 2012, 88, 90-96.	3.9	41
22	The impact of the relaxivity definition on the quantitative measurement of glycosaminoglycans in cartilage by the MRI dGEMRIC method. Magnetic Resonance in Medicine, 2010, 63, 25-32.	3.0	40
23	Anisotropic analysis of multiâ€component T <sub>2</sub> and T <sub>1ï</sub> relaxations in achilles tendon by NMR spectroscopy and microscopic MRI. Journal of Magnetic Resonance Imaging, 2013, 38, 625-633.	3.4	40
24	Imaging velocity profiles: Flow through an abrupt contraction and expansion. AICHE Journal, 1992, 38, 1408-1420.	3.6	39
25	On the measurement of multi-component T2 relaxation in cartilage by MR spectroscopy and imaging. Magnetic Resonance Imaging, 2010, 28, 537-545.	1.8	38
26	Averaged and Depth-Dependent Anisotropy of Articular Cartilage by Microscopic Imaging. Seminars in Arthritis and Rheumatism, 2008, 37, 317-327.	3.4	37
27	Strainâ€dependent <i>T</i> <sub>1</sub> relaxation profiles in articular cartilage by MRI at microscopic resolutions. Magnetic Resonance in Medicine, 2011, 65, 1733-1737.	3.0	35
28	Depth and orientational dependencies of MRI T2 and T1ϕsensitivities towards trypsin degradation and Gd-DTPA2â^' presence in articular cartilage at microscopic resolution. Magnetic Resonance Imaging, 2012, 30, 361-370.	1.8	35
29	Quantitative zonal differentiation of articular cartilage by microscopic magnetic resonance imaging, polarized light microscopy, and Fourierâ€transform infrared imaging. Microscopy Research and Technique, 2013, 76, 625-632.	2.2	35
30	Modifications of orientational dependence of microscopic magnetic resonance imaging T2 anisotropy in compressed articular cartilage. Journal of Magnetic Resonance Imaging, 2005, 22, 665-673.	3.4	33
31	Experimental issues in the measurement of multi-component relaxation times in articular cartilage by microscopic MRI. Journal of Magnetic Resonance, 2013, 235, 15-25.	2.1	32
32	"One-shot―velocity microscopy: NMR imaging of motion using a single phase-encoding step. Magnetic Resonance in Medicine, 1992, 23, 138-153.	3.0	31
33	Anisotropic properties of bovine nasal cartilage. Microscopy Research and Technique, 2012, 75, 300-306.	2.2	30
34	Macromolecular Concentrations in Bovine Nasal Cartilage by Fourier Transform Infrared Imaging and Principal Component Regression. Applied Spectroscopy, 2010, 64, 1199-1208.	2.2	29
35	Analysis of multi-exponential relaxation data with very short components using linear regularization. Journal of Magnetic Resonance, 2004, 167, 36-41.	2.1	27
36	Polarized IR microscopic imaging of articular cartilage. Physics in Medicine and Biology, 2007, 52, 4601-4614.	3.0	26

#	Article	IF	CITATIONS
37	Topographical variations of the strain-dependent zonal properties of tibial articular cartilage by microscopic MRI. Connective Tissue Research, 2014, 55, 205-216.	2.3	26
38	Effect of phosphate electrolyte buffer on the dynamics of water in tendon and cartilage. NMR in Biomedicine, 2009, 22, 158-164.	2.8	25
39	Morphological Changes in Articular Cartilage Due to Static Compression: Polarized Light Microscopy Study. Connective Tissue Research, 2007, 48, 76-84.	2.3	24
40	Further studies on the anisotropic distribution of collagen in articular cartilage by μMRI. Magnetic Resonance in Medicine, 2011, 65, 656-663.	3.0	23
41	Proteoglycan concentrations in healthy and diseased articular cartilage by Fourier transform infrared imaging and principal component regression. Spectrochimica Acta - Part A: Molecular and Biomolecular Spectroscopy, 2014, 133, 825-830.	3.9	23
42	Determination of Zonal Boundaries in Articular Cartilage Using Infrared Dichroism. Applied Spectroscopy, 2007, 61, 1404-1409.	2.2	22
43	Topographical variations in the polarization sensitivity of articular cartilage as determined by polarization-sensitive optical coherence tomography and polarized light microscopy. Journal of Biomedical Optics, 2008, 13, 054034.	2.6	21
44	Quantitative Determination of Morphological and Territorial Structures of Articular Cartilage from Both Perpendicular and Parallel Sections by Polarized Light Microscopy. Connective Tissue Research, 2011, 52, 512-522.	2.3	21
45	The effects of mechanical loading and gadolinium concentration on the change of T1 and quantification of glycosaminoglycans in articular cartilage by microscopic MRI. Physics in Medicine and Biology, 2013, 58, 4535-4547.	3.0	20
46	T1ï•Magnetic Resonance Imaging for Detection of Early Cartilage Changes in Knees of Asymptomatic Collegiate Female Impact and Nonimpact Athletes. Clinical Journal of Sport Medicine, 2014, 24, 218-225.	1.8	19
47	Quantitative measurement of T2, T1ϕand T1 relaxation times in articular cartilage and cartilage-bone interface by SE and UTE imaging at microscopic resolution. Journal of Magnetic Resonance, 2018, 297, 76-85.	2.1	19
48	Depth-dependent anisotropy of proteoglycan in articular cartilage by Fourier transform infrared imaging. Vibrational Spectroscopy, 2011, 57, 338-341.	2.2	18
49	Molecular origin of a loading-induced black layer in the deep region of articular cartilage at the magic angle. Journal of Magnetic Resonance Imaging, 2015, 41, 1281-1290.	3.4	16
50	Imaging the velocity profiles in tubeless siphon flow by NMR microscopy. Journal of Magnetic Resonance, 2003, 164, 365-368.	2.1	15
51	Fourier-transform infrared anisotropy in cross and parallel sections of tendon and articular cartilage. Journal of Orthopaedic Surgery and Research, 2008, 3, 48.	2.3	15
52	Chemical visualization of individual chondrocytes in articular cartilage by attenuated-total-reflection Fourier Transform Infrared Microimaging. Biomedical Optics Express, 2011, 2, 937.	2.9	15
53	Orientational dependent sensitivities of T2 and T1ï•towards trypsin degradation and Gd-DTPA2â^' presence in bovine nasal cartilage. Magnetic Resonance Materials in Physics, Biology, and Medicine, 2012, 25, 297-304.	2.0	15
54	Compressed sensing in quantitative determination of GAG concentration in cartilage by microscopic MRI. Magnetic Resonance in Medicine, 2018, 79, 3163-3171.	3.0	15

#	Article	IF	CITATIONS
55	MRI properties of a unique hypo-intense layer in degraded articular cartilage. Physics in Medicine and Biology, 2015, 60, 8709-8721.	3.0	14
56	Depth-Dependent Glycosaminoglycan Concentration in Articular Cartilage by Quantitative Contrast-Enhanced Micro–Computed Tomography. Cartilage, 2015, 6, 216-225.	2.7	14
57	Direct Visualisation of the Depth-Dependent Mechanical Properties of Full-Thickness Articular Cartilage. Open Journal of Orthopedics, 2012, 02, 34-39.	0.1	14
58	Effects of Cryopreservation on the Depth-Dependent Elastic Modulus in Articular Cartilage and Implications for Osteochondral Grafting. Journal of Biomechanical Engineering, 2015, 137, 054502.	1.3	13
59	Reversed laminar appearance of articular cartilage by T1â€weighting in 3D fatâ€suppressed spoiled gradient recalled echo (SPGR) imaging. Journal of Magnetic Resonance Imaging, 2010, 32, 733-737.	3.4	12
60	Fourier Transform Infrared Microscopic Imaging and Fisher Discriminant Analysis for Identification of Healthy and Degenerated Articular Cartilage. Chinese Journal of Analytical Chemistry, 2015, 43, 518-522.	1.7	12
61	Loading-induced changes on topographical distributions of the zonal properties of osteoarthritic tibial cartilage – A study by magnetic resonance imaging at microscopic resolution. Journal of Biomechanics, 2015, 48, 3625-3633.	2.1	12
62	Changes in Proton Dynamics in Articular Cartilage Caused by Phosphate Salts and Fixation Solutions. Cartilage, 2010, 1, 55-64.	2.7	11
63	Experimental Influences in the Accurate Measurement of Cartilage Thickness in MRI. Cartilage, 2019, 10, 278-287.	2.7	11
64	Orientational dependence of trimethyl ammonium signal in human muscles by 1H magnetic resonance spectroscopic imaging. Magnetic Resonance Imaging, 2005, 23, 97-104.	1.8	10
65	Discrimination of healthy and osteoarthritic articular cartilages by Fourier transform infrared imaging and partial least squares-discriminant analysis. Journal of Biomedical Optics, 2015, 20, 060501.	2.6	10
66	Discrimination of healthy and osteoarthritic articular cartilage by Fourier transform infrared imaging and Fisher's discriminant analysis. Biomedical Optics Express, 2016, 7, 448.	2.9	10
67	Topographical variations in zonal properties of canine tibial articular cartilage due to early osteoarthritis: a study using 7-T magnetic resonance imaging at microscopic resolution. Magnetic Resonance Materials in Physics, Biology, and Medicine, 2016, 29, 681-690.	2.0	10
68	Functional properties of chondrocytes and articular cartilage using optical imaging to scanning probe microscopy. Journal of Orthopaedic Research, 2018, 36, 620-631.	2.3	10
69	Significant differences in proton trimethyl ammonium signals between human gastrocnemius and soleus muscle. Journal of Magnetic Resonance Imaging, 2004, 19, 617-622.	3.4	9
70	Depthâ€dependent anisotropies of amides and sugar in perpendicular and parallel sections of articular cartilage by Fourier transform infrared imaging. Microscopy Research and Technique, 2011, 74, 122-132.	2.2	9
71	Spin locking in liquid entrapped in nanocavities: Application to study connective tissues. Journal of Magnetic Resonance, 2019, 299, 66-73.	2.1	9
72	Spin-lattice relaxation in liquid entrapped in a nanocavity. Journal of Magnetic Resonance, 2020, 311, 106669.	2.1	9

#	Article	IF	CITATIONS
73	High spatial resolution in vivo 2D 1H magnetic resonance spectroscopic imaging of human muscles with a band-selective technique. Magnetic Resonance Imaging, 2001, 19, 1091-1096.	1.8	8
74	Anisotropy of transverse and longitudinal relaxations in liquids entrapped in nano- and micro-cavities of a plant stem. Journal of Magnetic Resonance, 2021, 331, 107051.	2.1	8
75	Meniscus Induced Cartilaginous Damage and Non-linear Gross Anatomical Progression of Early-stage Osteoarthritis in a Canine Model. The Open Orthopaedics Journal, 2016, 10, 690-705.	0.2	8
76	Spectral pattern of total creatine and trimethyl ammonium in multiple sclerosis. Magnetic Resonance Imaging, 2004, 22, 427-429.	1.8	7
77	Topographical and depth-dependent glycosaminoglycan concentration in canine medial tibial cartilage 3 weeks after anterior cruciate ligament transection surgery—a microscopic imaging study. Quantitative Imaging in Medicine and Surgery, 2016, 6, 648-660.	2.0	6
78	COMPARISON OF MACROMOLECULAR COMPONENT DISTRIBUTIONS IN OSTEOARTHRITIC AND HEALTHY CARTILAGES BY FOURIER TRANSFORM INFRARED IMAGING. Journal of Innovative Optical Health Sciences, 2013, 06, 1350048.	1.0	5
79	Detection of early osteoarthritis in canine knee joints 3 weeks post ACL transection by microscopic MRI and biomechanical measurement. Journal of Orthopaedic Surgery, 2018, 26, 230949901877835.	1.0	5
80	Introduction to Cartilage. New Developments in NMR, 2016, , 1-43.	0.1	5
81	Relaxation Anisotropy as a Possible Marker for Macromolecular Orientations in Articular Cartilage. , 0, , 351-362.		4
82	Image interpolation improves the zonal analysis of cartilage T2 relaxation in MRI. Quantitative Imaging in Medicine and Surgery, 2017, 7, 227-237.	2.0	4
83	Quantitative µMRI and PLM study of rabbit humeral and femoral head cartilage at subâ€10 µm resolutions. Journal of Orthopaedic Research, 2020, 38, 1052-1062.	2.3	4
84	Topographical and zonal patterns of T2 relaxation in osteoarthritic tibial cartilage by low- and high-resolution MRI. Magnetic Resonance Imaging, 2021, 78, 98-108.	1.8	4
85	Determining the internal orientation, degree of ordering, and volume of elongated nanocavities by NMR: Application to studies of plant stem. Journal of Magnetic Resonance, 2022, 341, 107258.	2.1	4
86	The influences of different spatial resolutions on the characteristics of T2 relaxation times in articular cartilage: A coarseâ€graining study of the microscopic magnetic resonance imaging data. Microscopy Research and Technique, 2016, 79, 754-765.	2.2	3
87	Dynamics of Zeeman and dipolar states in the spin locking in a liquid entrapped in nano-cavities: Application to study of biological systems. Journal of Magnetic Resonance, 2021, 325, 106933.	2.1	3
88	The interface region between articular cartilage and bone by <scp>μMRI</scp> and <scp>PLM</scp> at microscopic resolutions. Microscopy Research and Technique, 2022, 85, 1483-1493.	2.2	3
89	Structural differences between immature and mature articular cartilage of rabbits by microscopic MRI and polarized light microscopy. Journal of Anatomy, 2022, 240, 1141-1151.	1.5	3
90	Physical Properties of Cartilage by Relaxation Anisotropy. New Developments in NMR, 2016, , 145-175.	0.1	2

#	Article	IF	CITATIONS
91	Resolutionâ€dependent influences of compressed sensing in quantitative T2 mapping of articular cartilage. NMR in Biomedicine, 2020, 33, e4260.	2.8	2
92	Fourier-transform infrared spectroscopic imaging of articular cartilage and biomaterials: A review. Trends in Applied Spectroscopy, 2013, 10, 1-23.	0.0	2
93	Averaged Properties of Articular Cartilage from Multidisciplinary Microscopic Imaging Study. , 2005, 2005, 3161-4.		1
94	Morphological Changes of Chondrocytes in Compressed Articular Cartilage Using Polarized Light Microscopy. International Conference on Bioinformatics and Biomedical Engineering: [proceedings] International Conference on Bioinformatics and Biomedical Engineering, 2010, , .	0.0	1
95	The First Study of Cartilage by Magnetic Resonance. Cartilage, 2016, 7, 293-297.	2.7	1
96	Structural Morphology of Rabbit Patella and Suprapatella Cartilage by Microscopic MRI and Polarized Light Microscopy. Cartilage, 2021, 13, 356S-366S.	2.7	1
97	Imaging the Depth-Dependent Anisotropies in Articular Cartilage by Multidisciplinary Microscopies (μMRI, PLM, FTIRI). , 2007, , .		0
98	Concentration determination of collagen and proteoglycan in bovine nasal cartilage by Fourier transform infrared imaging and PLS. Proceedings of SPIE, 2014, , .	0.8	0
99	Anisotropy of transverse spin relaxation in H2O-D2O liquid entrapped in Nanocavities: application to studies of connective tissues. Hyperfine Interactions, 2021, 242, 1.	0.5	0
100	Location-Specific Study of Young Rabbit Femoral Cartilage by Quantitative µMRI and Polarized Light Microscopy. Cartilage, 2022, 13, 194760352210851.	2.7	0
101	CHAPTER 13. The Influence of Specimen and Experimental Conditions on NMR and MRI of Cartilage. New Developments in NMR, 0, , 347-372.	0.1	0
102	CHAPTER 16. Loading-Induced Changes in Cartilage Studied by NMR and MRI. New Developments in NMR, 0, , 433-454.	0.1	0
103	CHAPTER 17. The Critical Role of High Imaging Resolution in MRI of Cartilage—The MRI Microscope. New Developments in NMR, 0, , 455-470.	0.1	0
104	CHAPTER 18. Multicomponent Relaxation in NMR and MRI of Cartilage. New Developments in NMR, 0, , 471-493.	0.1	0
105	CHAPTER 21. Complementary Imaging in MRI of Cartilage. New Developments in NMR, 0, , 552-574.	0.1	0
106	Microscopic Imaging of Structured Macromolecules in Articular Cartilage. , 0, , 303-314.		0